PRACTICAL ELECTRON MICROSCOPY IN MATERIALS SCIENCE

1 Monograph One
The operation and calibration of the electron microscope

J W Edington

Philips Technical Library

Monographs in Practical Electron Microscopy in Materials Science

1

THE OPERATION AND CALIBRATION OF THE ELECTRON MICROSCOPE

J. W. EDINGTON

Department of Metallurgy and Materials Science, University of Cambridge, Cambridge, England

M

SBN 333 18133 6

First published 1974 by
THE MACMILLAN PRESS LTD
London and Basingstoke
Associated companies in New York, Melbourne,
Dublin, Johannesburg and Madras

PHILIPS

Filmset at The Universities Press, Belfast, Northern Ireland
and printed by Thomson Litho Ltd., East Kilbride, Scotland.

PREFACE

This is the first of a series of monographs on electron microscopy aimed at users of the equipment. They are written both as texts and sources of reference emphasising the applications of electron microscopy to the characterisation of materials. The flexible monograph format will enable both the student and the professional scientist to extract the required information easily. In this context the series should be useful in specialist undergraduate and postgraduate lecture courses and as an introduction to the technique for professional scientists.

In some places the author has referred the reader to material appearing in other monographs in this series. The following three monographs are in preparation:

2—Electron Diffraction in the Electron Microscope,

3—Interpretation of Transmission Electron Micrographs and

4—Typical Electron Microscope Investigations.

Subsequent monographs in the series will cover quantitative metallography, together with aspects of design of electron microscopes.

CONTENTS

Preface

1.1 INTRODUCTION 1

1.2 LENS DEFECTS 1

1.3 RESOLUTION 2

1.4 IMPORTANT ASPECTS OF MICROSCOPE OPERATION AND ALIGNMENT 4
- 1.4.1 Alignment of the Objective Lens Axis 4
- 1.4.2 Objective Astigmatism Correction 5
- 1.4.3 Illumination Conditions 7
- 1.4.4 Axis-centred Specimen Tilt 7

1.5 THE FORMATION OF DIFFRACTION PATTERNS AND IMAGES 7
- 1.5.1 Selected Area Diffraction 8
- 1.5.2 Bright and Dark Field Images 10
- 1.5.3 Weak Beam Images 12
- 1.5.4 Multiple Dark Field Images 13
- 1.5.5 Phase Contrast Images 14

1.6 STEREO MICROSCOPY 18

1.7 MAGNETIC SPECIMENS 18
- 1.7.1 Magnetic Correction 18
- 1.7.2 Lorentz Microscopy 19

1.8 BEAM-SENSITIVE MATERIALS 19

1.9 LOW ANGLE DIFFRACTION 21

1.10 ANALYSIS OF PLATES 21

1.11 CALIBRATION OF THE MICROSCOPE 21
- 1.11.1 Image Magnification 22
  - 1.11.1.1 Diffraction grating replicas 22
  - 1.11.1.2 Direct lattice images 22
- 1.11.2 Diffraction Pattern Magnification 23
- 1.11.3 Image-diffraction Pattern Rotation 23
- 1.11.4 Errors in Use of Permanent Calibrations 24
- 1.11.5 Additional Measurements 25
  - 1.11.5.1 Accelerating voltage 26
  - 1.11.5.2 Specimen drift rate 26
  - 1.11.5.3 Specimen contamination rate 26
  - 1.11.5.4 The position of the specimen tilt axis and sense of tilt 26
  - 1.11.5.5 Focal increments of the objective lens 26
  - 1.11.5.6 Beam current 26

1.12 RESOLUTION TESTS 27

References 29

APPENDIX 12. PREPARATION OF HIGH-RESOLUTION TEST SPECIMENS 31

A12.1 Single-crystal (100) Gold Films 31

A12.2 Partially Graphitised Carbon Black 31

A12.3 Replicas for Point-to-point resolution tests 31

Appendix 12. References 33

APPENDIX 13. HOLEY CARBON REPLICAS 34

Appendix 13. References 34

1. THE OPERATION AND CALIBRATION OF THE ELECTRON MICROSCOPE

1.1 Introduction

An electron microscope uses a series of magnetic lenses to focus an electron beam that is accelerated, by a high potential, through the specimen *in vacuo*. The main features of a modern microscope are shown schematically in figure 1.1. An electrically heated tungsten filament, at a selected negative potential 20–100 kV, is mounted on a ceramic insulator behind a Wehnelt cap with a central hole. The electrons emitted by the filament are accelerated to earth and are focussed, via a double condenser lens system with field-limiting apertures, onto the specimen. An image or diffraction pattern from the specimen is obtained on a fluorescent screen via a three- or a four-lens (illustrated) magnification system. Image contrast may be enhanced by the use of an objective aperture, and the area for diffraction may be selected by a selected area aperture. The image is focussed with the objective lens and magnification is controlled by the excitation of the intermediate and/or diffraction lens. The depth of field of the instrument is such that the top and bottom of the specimen are simultaneously in focus while its depth of focus enables the plate or film camera to be situated up to 50 cm above or below the viewing screen.

There are limitations on the performance of an electron microscope because of lens defects. Nevertheless, in general the accuracy of operation and calibration of the instrument controls the quality of electron micrographs, and the precision with which they can be analysed quantitatively. In addition, the type of information required from the specimen controls the operation procedure employed, and therefore to some extent the details of the information obtained. It is our purpose here to describe the important lens defects and their influence on instrumental performance, together with the various operation modes and calibration requirements of the microscope. Some of the terminology used here is defined in subsequent sections. In particular, that associated with the diffraction pattern may be found in the early parts of section 2.

1.2 Lens Defects

Like glass lenses, all electromagnetic lenses suffer from defects such as coma, barrel or pincushion distortion, astigmatism, chromatic and spherical aberration which are discussed in detail by Haine (1961). From the operator's standpoint the last three are the most important in relation to the objective lens because they determine the resolution of the electron microscope.

Spherical aberration is particularly important because there is no convenient way of correcting it. This defect is shown schematically in figure 1.2(a). Electrons leaving a point P on the optic axis of the specimen at the object are refocussed at P″ instead of P′. Consequently, in the image plane the point is imaged as a disc; its radius Δr_s is given by

$$\Delta r_s = C_s \beta^3 \tag{1.1}$$

where C_s is the spherical aberration constant and is typically 1 or 2 mm for an objective lens. Thus the point resolution deteriorates rapidly with increasing β, that is lens aperture.

Chromatic aberration arises because of the energy, and therefore wavelength, spread of the electron beam. Instabilities in accelerating voltage or lens current could be contributory factors, but both are negligible because of the high stability of modern power supplies. Although there is a small energy spread ~ 3 eV in the electron beam leaving the tungsten filament in the electron gun, the major factor is the large energy loss $\Delta E = 5$–50 eV suffered by many electrons on passing through the specimen. In effect the focal length of the lens varies with the electron energy, see figure 1.2(b). A disc of confusion, radius Δr_c, is produced, given by

$$\Delta r_c = C_c \beta \frac{\Delta E}{E} \tag{1.2}$$

where C_c is the chromatic aberration constant of the lens and is approximately equal to its focal length.

Astigmatism occurs when the lens exhibits different focal lengths, depending upon the plane of the ray paths. Thus, in figure 1.2(c), the rays travelling in plane A are focussed at P_A while those in plane B focus at P_B. Again a point on the object is imaged as a disc of confusion, radius Δr_A, given by

$$\Delta r_A = \Delta f_A \beta \tag{1.3}$$

where Δf_A is the maximum difference in focal

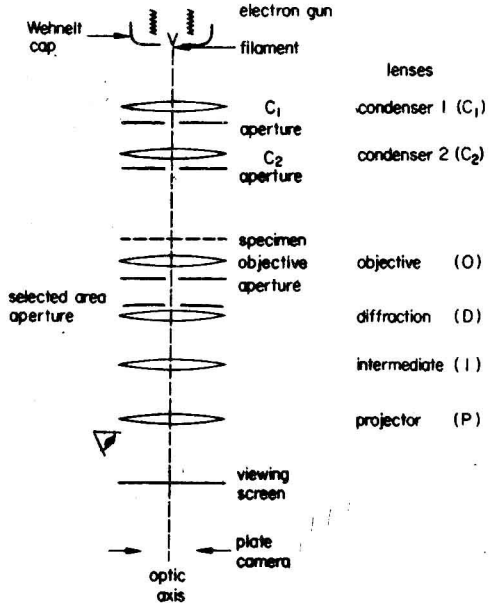

Figure 1.1 A schematic diagram showing the important components of the microscope

length arising from astigmatism. This defect may be corrected using electromagnetic astigmators that produce a small controllable magnetic field. Astigmatism of the condenser lens system is important because it reduces the coherence of the beam, while that of the objective lens is important because it can cause a serious loss in image resolution.

Condenser astigmatism is manifested by an elliptical illumination spot when the condenser 2 is defocussed. The astigmator is adjusted to make the defocussed spot circular. Objective astigmatism is manifested by streaking in one direction of fine detail of the image, compare figures 1.3(a), (b), and may be corrected using the procedure outlined in section 1.4.2.

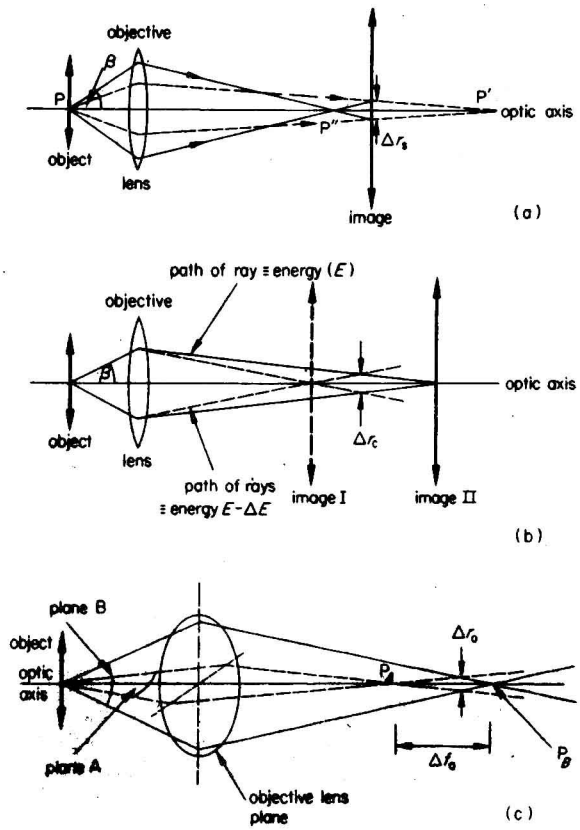

Figure 1.2 Objective lens aberrations: (a) spherical, (b) chromatic, (c) astigmatism

1.3 Resolution

There are two forms of resolution of interest in electron microscopy. The first is the instrument resolution, and the second is the effective resolution for a particular type of specimen.

Consider first instrument resolution, which is a function of the aberrations of the objective lens. Referring to equation (1.1) it is clear that spherical aberration demands the use of very small apertures to maximise resolution. However, if the aperture size is reduced too far, diffraction effects at the aperture become a limiting factor. In this context it was shown by Airy (1835) that diffraction by a lens aperture causes a point source to be imaged as a bright central disc, known as Airy's disc, surrounded by a number of fainter rings. Thus the intensity distribution in the image plane for two point sources in the object plane is that shown in figure 1.4(a) for a lens of angular aperture β. As S_1 and S_2 approach each other the disc images in the image plane overlap, see figure 1.4(b)–(d). It is shown in books on physical optics, for example, Jenkins and White (1951) that the closest distance of approach at which both discs can be resolved is given by the Rayleigh criterion that the central minimum, figure 1.4(e), has an intensity of 0.81 of the maximum. The point-to-point resolution limit is then

$$\Delta r_d = \frac{0.61\lambda}{\beta} \tag{1.4}$$

Since increasing the aperture size increases resolution according to equation (1.4) but decreases it according to equation (1.1), there is an optimum aperture size that minimises their sum, that is

$$\beta \approx \left(\frac{\lambda}{C_s}\right)^{1/4} \tag{1.5}$$

which gives a maximum resolution

$$\Delta r_{min} \approx \lambda^{3/4} C_s^{1/4} \tag{1.6}$$

Using this approach typical values of optimum aperture diameter ($= 2\beta f$) may be calculated for the EM300 and these are given in table 1.1 for the high-resolution stage and pole pieces.

Consideration of the values of the optimum resolving power at 100 kV (see table 1.1) indicates that, before spherical aberration becomes the factor limiting resolution in the EM300, it is necessary to correct for astigmatism to the extent

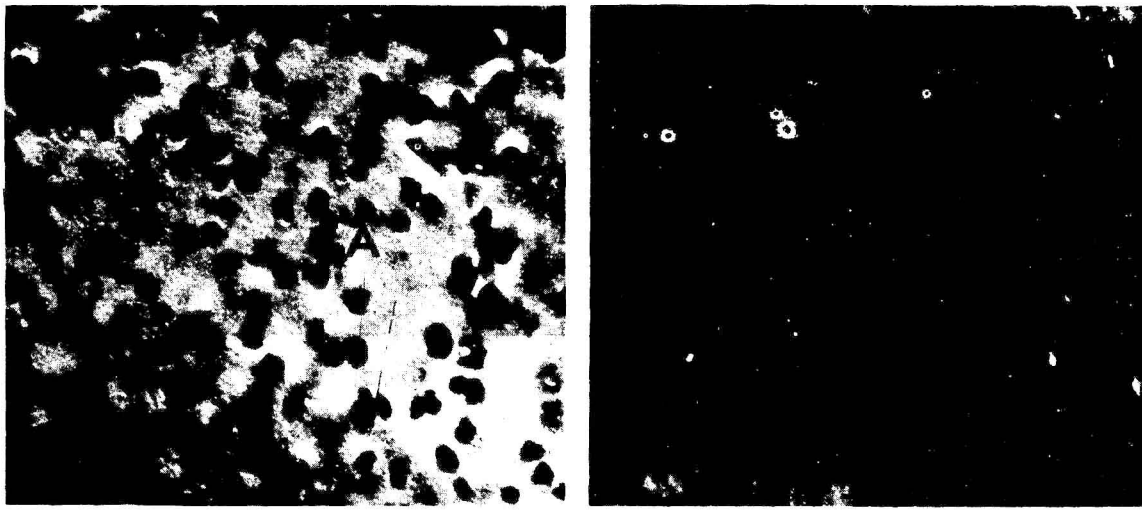

Figure 1.3 Bright field images of an aged Al–6% Zn–3% Mg alloy, showing η precipitates. Astigmatism (a) correctly, (b) incorrectly adjusted. The points marked A are the same in both figures

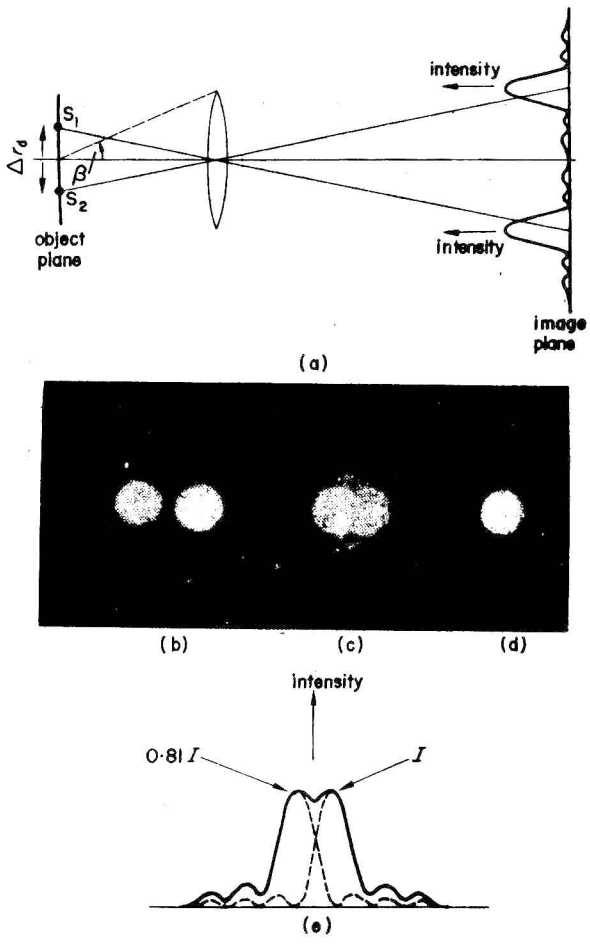

Figure 1.4 (a) The formation of two Airy disc images of point sources S_1, S_2 through diffraction at the objective aperture (angle β), (b) clearly resolved Airy discs, (c) just resolved, (d) unresolved, (e) the situation corresponding to (c), that is Rayleigh criterion such that the intensity in the centre is 0.81 of the maximum

* For details of these processes see Raimes (1961).

that $\Delta r_A = 2.3$ Å. In practice this means that one must be able to distinguish a variation in Fresnel fringe spacings of the order of 4 Å in 12 Å, see section 1.4.2. This conclusion is derived for a resolving power of $\Delta r_{min} = 2.3$ Å, $\beta = 10^{-3}$ rad to obtain a value for Δf_a and then assuming $X_{max} =$ 12 Å in equation (1.9). Clearly such accuracy of astigmatism correction will only be achieved by special efforts and a more realistic level of point-to-point resolving power for electron microscopes is $\gtrsim 5$ Å.

The influence of the specimen is generally to degrade resolution through chromatic aberration effects arising because many electrons lose small amounts of energy in passing through the specimen. As an example consider the typical case of a thin metal foil of thickness approximately 50% of the maximum useful penetration. Perhaps up to 40% of the electrons included in the final image will have lost energy in amounts of up to 50 eV by plasma or single-electron* excitation in the specimen. Substituting in equation (1.2) values of $C_c = 3.3$ mm for the goniometer stage of the EM300, and E is 100 kV with $\beta = 5 \times 10^{-3}$ rad, r_c is 25 Å if the energy loss ΔE is only 15 eV. Thus, in a typical thin foil it is the specimen that limits resolution unless very thin regions are used to minimise energy losses.

Finally, it is important to note that, when attempting to produce high-resolution images, for example 5 Å point-to-point, objective aperture diffraction effects can be important. The diameter of the Airy disc produced by the objective aperture is $\sim 1.2\lambda f/D$, where f is the focal length of the lens and D is the aperture diameter. Typical values for a range of objective aperture sizes are given in table 1.2 for the EM300/301.

Table 1.1 Optimum objective aperture diameters (D_{opt}) for maximum resolution, assuming spherical aberration is the controlling process for the high-resolution stage[a] of the EM300/301, C_s = 1.6 mm

Accelerating voltage (kV)	Wavelength (Å)	D_{opt} (μm)	Optimum resolving power (Å)	Theoretical resolving power for actual objective aperture diameters (μm)				
				30	25	20	15	10
20	0.086	33	4.3	4.8	5.8	7.2	9.6	14.5
40	0.060	30	3.3	3.3	4.0	5.0	6.7	10.2
60	0.048	29	2.8	2.8	3.2	4.0	5.3	8.1
80	0.042	28	2.5	2.5	2.7	3.5	4.6	7.1
100	0.037	27	2.3	2.3	2.5	3.1	4.1	6.3

[a] Multiply these values by 1.55 for the goniometer stage.

These values represent the practical resolution limit of the microscope for these aperture sizes and interpretation of image detail on a finer scale than the values in table 1.2 is quite uncertain. Thus the practice of using small objective apertures to reduce the inelastic scattering contribution to bright field images, or to exclude closely spaced spots where forming centred dark field images, can seriously reduce resolution and complicate interpretation of fine scale microstructural effects.

Resolution tests are discussed in section 1.12.

1.4 Important Aspects of Microscope Operation and Alignment

The following three factors are the most important in controlling image quality.

(1) Alignment of the objective lens axis.
(2) Adjustment of objective astigmatism.
(3) Illumination conditions.

The additional following factor greatly eases operation of the instrument for materials science studies.

(4) Axis-centred specimen tilting.

The principles behind (1)–(4) above are described in the following sections. It is important to realise that, although the specimen itself may reduce resolution through chromatic aberration (section 1.2), it is still necessary to align the instrument carefully, paying particular attention to (1)–(3) above because all factors are additive in determining final resolution.

Table 1.2 Values of the diameter of the Airy disc produced by diffraction from the objective aperture of the EM300/301

Objective aperture diameter (μm)	Diameter of Airy disc (Å)	
	High-resolution stage f = 1.6 mm	Goniometer stage f = 4.1 mm
40	1.8	4.5
30	2.4	6.1
20	3.5	9.1
10	7.1	18.2

1.4.1 *Alignment of the Objective Lens Axis*

Misalignment of this lens seriously reduces the resolving power of the instrument because of increased spherical aberration, and sensitivity to chromatic aberration. This alignment must therefore be performed extremely carefully. The influence of an off-axis beam entering the objective lens is shown in figure 1.5(a). Here the object ABC forms an image A′B′C′ (solid ray paths) for a given objective lens setting. If, however, the objective lens setting is changed the image will be A″B″C″ (dashed ray paths) smaller than A′B′C′ but central about the undeviated beam BB′. In addition, there will be a rotation of the image because of the helical path of the electrons through the lens. Essentially, the image rotates about a point (rotation centre) off the centre of the viewing screen when the objective lens current is changed, see figure 1.5(b). Depending upon the microscope, the beam may be made to travel down the optic axis of the lens by either tilting the incident illumination, figure 1.6(a), or adjusting the objective lens pole piece, that is the optic axis of the lens, figure 1.6(b), (c). This is achieved by adjusting either of these

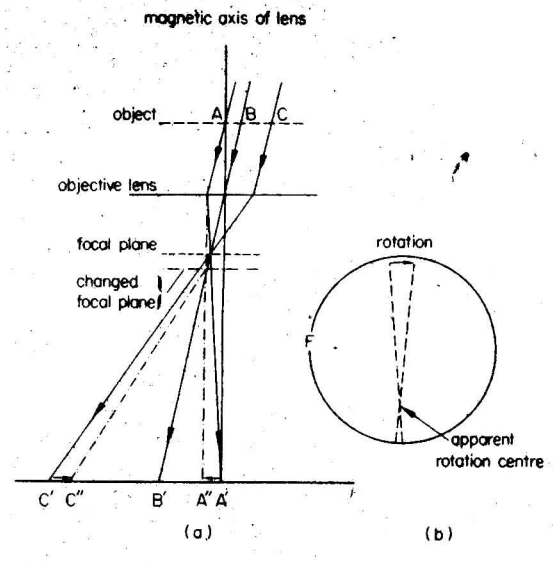

Figure 1.5 The effect of non-axial illumination of the objective lens: (a) showing the sweep of the image, (b) the combined effect of sweep and rotation of the image on the viewing screen

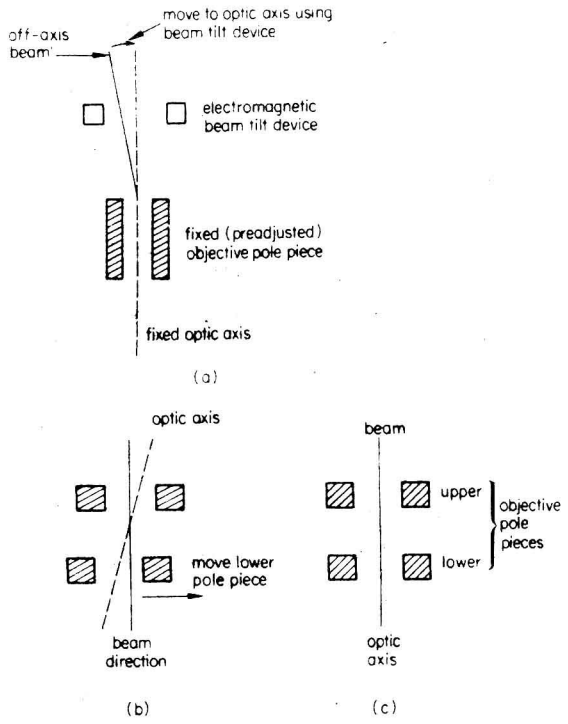

Figure 1.6 The correction of non-axial objective lens illumination by (a) electromagnetic beam tilt, (b), (c) movement of the lower objective lens pole piece for an immersion lens

controls to move the rotation centre to the centre of the viewing screen. The rotation centre may be defined by defocussing the objective lens and observing the centre of rotation of the image.

1.4.2 *Objective Astigmatism Correction*

Image resolution is very sensitive to objective astigmatism. Consequently, it is important to correct it carefully.

Conventionally, objective astigmatism is adjusted using the Fresnel fringes near the edge of a small hole viewed with the objective lens overfocussed.

Figure 1.7(a) shows schematically the occurrence of diffraction at the edge of a carbon film. Consider a plane wave scattered at A through an angle β. Interference between the wave and the undeviated wave at B is described by the path difference AB − Z, that is

$$X\beta = \frac{X^2}{Z} \tag{1.7}$$

which has a maximum when it is an integral number of wavelengths $n\lambda$, that is

$$X = (n\lambda D)^{1/2} \tag{1.8}$$

The contrast of the fringes is only appreciable for very small values of n because the amplitude of the scattered wave falls off as 1/AB. If $n < 2$, the objective lens must be defocussed by $Z \approx 1\ \mu m$ to observe a fringe spacing of ~10 Å. The width of the first dark fringe decreases on approaching focus where is disappears ($Z = 0$). For an astigmatic lens with differences in focal length as shown in figure 1.2(c), focus will be different around a hole and the fringe will disappear at some points before others. Consequently the objective lens may be overfocussed* when viewing a small, round hole in a thin carbon film until a dark fringe is observed, as shown in figure 1.7(b), then the objective astigmator adjusted until the fringe is uniform around the hole and disappears uniformly on approaching focus. Figure 1.7(c) shows a correctly compensated image. This adjustment is always performed at the highest magnification possible (> 100 000 × on the screen) using the binoculars to view the image. The anticontaminator should be used to minimise contamination which increases the thickness of the film and makes observation of the fringe more difficult.

The divergence of the incident beam is an important factor which limits the observation of Fresnel fringes. If there are two beams at an angle β' the two fringe systems will be out of step by $Z\beta'$, the separation of the geometric shadow in the focus plane, see figure 1.7(f). In order to observe a given fringe system $Z\beta'$ must be ≪ fringe spacing. For 10 Å fringes $\beta' \ll 10/Z$ and if $D = 1\ \mu m$ then $\beta' \ll 10^{-3}$ and if a narrower fringe is to be observed the divergence must be even smaller. Thus condenser 2 must be defocussed to decrease β' and to permit the observation of fringes.

Having obtained a photograph of the best corrected fringe, the residual astigmatism can be evaluated by measuring the maximum and minimum fringe width X_{max} and X_{min}. Then

$$\Delta f_a = \frac{1}{\lambda}(X_{max}^2 - X_{min}^2) \tag{1.9}$$

which may be used to evaluate the influence of the astigmatism on instrumental resolution.

When aiming for best resolution it is frequently necessary to correct for astigmatism on the specimen under study when a suitable hole may not be available. Such correction is required because the objective aperture itself can introduce additional astigmatism if it is not perfectly centred on the optic axis. In addition, astigmatism changes in the vicinity of specimen support grid bars. Under these circumstances it is best to correct astigmatism using the fine background image structure. This technique is illustrated in figure 1.7(g), (h). First the objective lens is focussed for minimum background contrast, figure 1.7(g). Any residual contrast then arises from variations in defocus of the objective lens from astigmatism which produces phase contrast as described in section 1.5.5. Then the objective astigmators are carefully adjusted for

* Overfocus is defined as an overexcited lens, that is focussed between the normal focal plane and the plane of the lens. Underfocus is an underexcited lens, that is focussed behind the normal plane of focus.

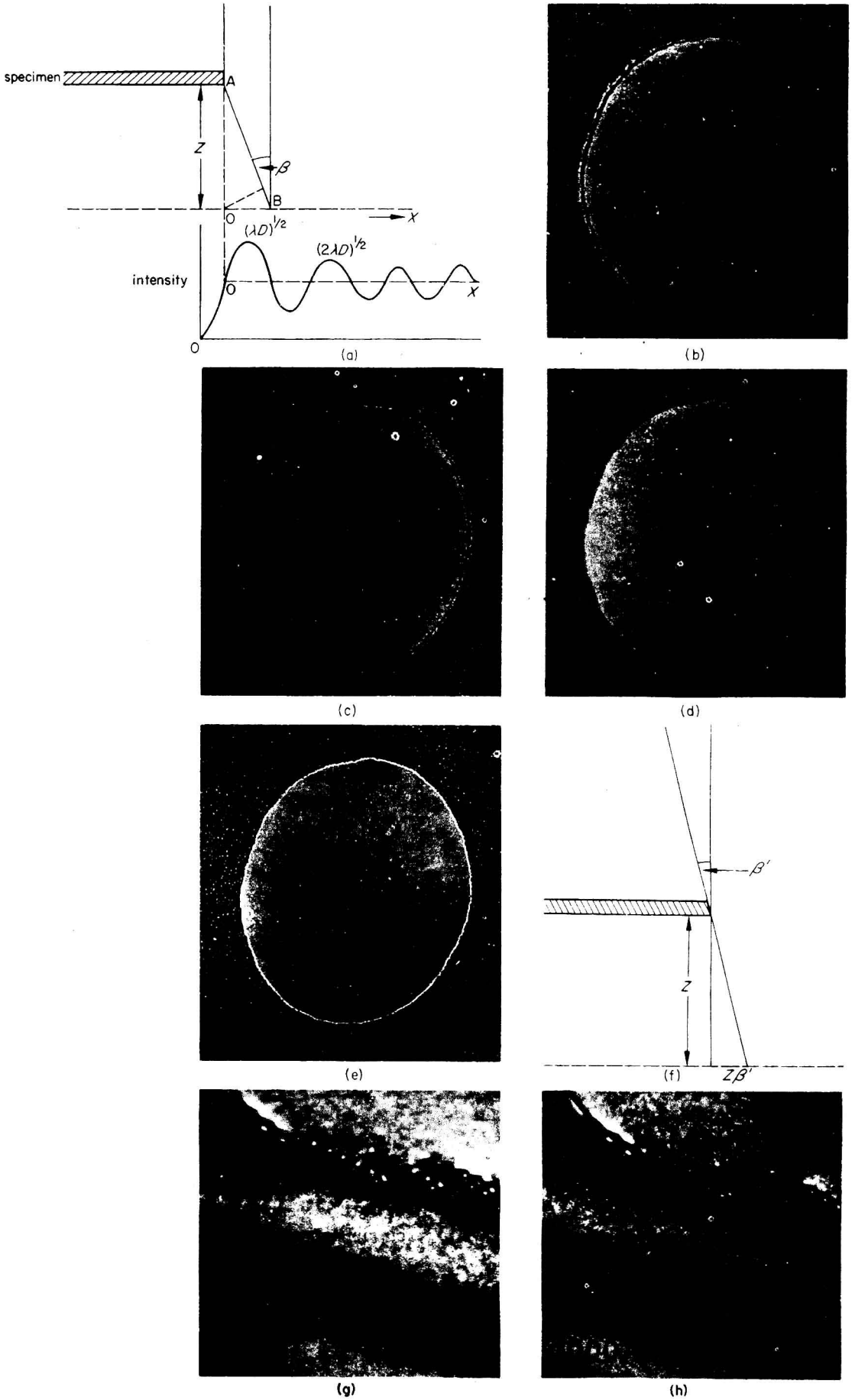

Figure 1.7 (a) The formation of Fresnel fringes at an edge, showing the intensity distribution at depth z below the specimen, (b) a hole in the carbon film showing the overfocus dark fringe for incorrectly and (c)–(e) overfocus, in-focus and underfocus images for correctly adjusted objective astigmatism, (f) the effect of incident beam convergence on Fresnel fringe formation, (g) in-focus image of molybdenum showing incorrectly adjusted objective astigmatism (this is an exaggerated example, significant maladjustment of astigmatism is present), (h) the same area with astigmatism correctly adjusted. Note the improvement in resolution on background.

minimum, but sharp, background contrast, figure 1.7(f), that is as uniform an objective focal length as possible.

This method is suitable for most crystalline specimens,* using the fine background structure of the image arising from the thin surface oxide layer usually present as for figure 1.7(g), (h). If image magnifications of $>100\,000\times$ on the screen are used the result is usually at least as good as the Fresnel fringe approach.

1.4.3 *Illumination Conditions*

The illumination conditions influence the quality of both images and diffraction patterns. As the beam intensity is increased, for example by weakening the excitation of condenser 1, the following effects occur.

(1) Carbon contamination increases.

(2) Local specimen heating increases, producing differential thermal expansion between specimen and support grid which causes more specimen drift.

(3) Electrical charging of the specimen may increase.

(4) The coherence of the illumination is reduced.

All of these effects reduce resolution in the image. Factors (1)–(3) above may be minimised by selecting minimum spot size using condenser 2 near focus, but this reduces the coherence of the illumination and therefore the resolution of the image. Consequently, choice of illumination conditions is a compromise. Thus the beam must be bright enough to keep exposure times $\lesssim 10$–15 s to minimise loss in resolution from specimen drift. However, as far as possible, condenser 2 should be defocussed to two or three times the minimum spot size to ensure adequate coherence of illumination.

Diffraction patterns should be obtained with condenser 2 well defocussed (two coarse clicks of potentiometer) to maximise sharpness.

1.4.4 *Axis-centred Specimen Tilt*

In most electron microscopes the field of view changes when the specimen is tilted which necessitates frequent re-centring of the area of interest using the specimen traverse controls. Thus it is impossible to tilt the specimen in the most convenient way, that is while observing its orientation in the diffraction pattern, because the diffraction pattern comes from a continually changing area of the specimen. However, some modern electron microscopes, such as the EM300/301, have provision for preventing this movement so that the field of view remains constant during specimen

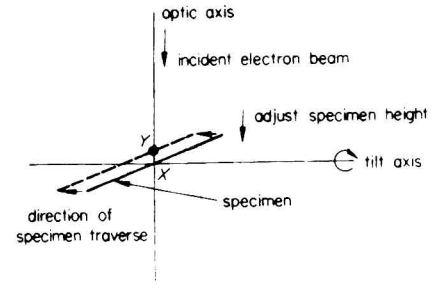

Figure 1.8 A schematic illustration of axis-centred tilt

tilts of $\pm 60°$. To achieve this, the area of the specimen viewed must be positioned at the point defined by the intersection of the optic axis and the tilt axis, as shown schematically in figure 1.8. The solid line indicates the position of the specimen with the field of view X illuminated by an electron beam traversing the optic axis. If the specimen is now translated to the position defined by the dashed line the new field of view will be Y which is now above the intersection of the tilt and optic axes. However, Y may be brought to this point by adjustment of the specimen height. Clearly for a microscope with this adjustment the objective lens is operated close to a standard setting, that is focussed on X. This greatly simplifies the calibration procedures outlined in sections 1.11.1, 1.11.2 and 1.11.3.

In order to achieve axis-centred tilting it is necessary to be able to adjust and to fix the specimen tilt axis until it coincides with the optic axis, then to adjust separately the specimen height. Note that if the specimen is tilted while in the dashed position the field of view of interest will move in or out of the plane of the paper.

1.5 The Formation of Diffraction Patterns and Images

The microscope may be operated to produce either a diffraction pattern from a specific region of the specimen ($\gtrsim 0.5$ μm in diameter) or one of several types of image. In all cases where quantitative information about the microstructure of the material is required, detailed correlation is made between the diffraction pattern and the image.

The essential features of the diffraction and image modes of operation can be explained in terms of a geometric optics treatment of the situation at the objective lens. Figure 1.9(a) shows an electron beam parallel to the optic axis and incident upon the specimen. The action of forming the image brings both the transmitted and the diffracted beam to a focus in the back focal plane of the objective lens. Thus a diffraction pattern is produced here.

* It may also be used for a carbon replica when it should be possible to obtain less contrast than is visible in figure 1.7(f).

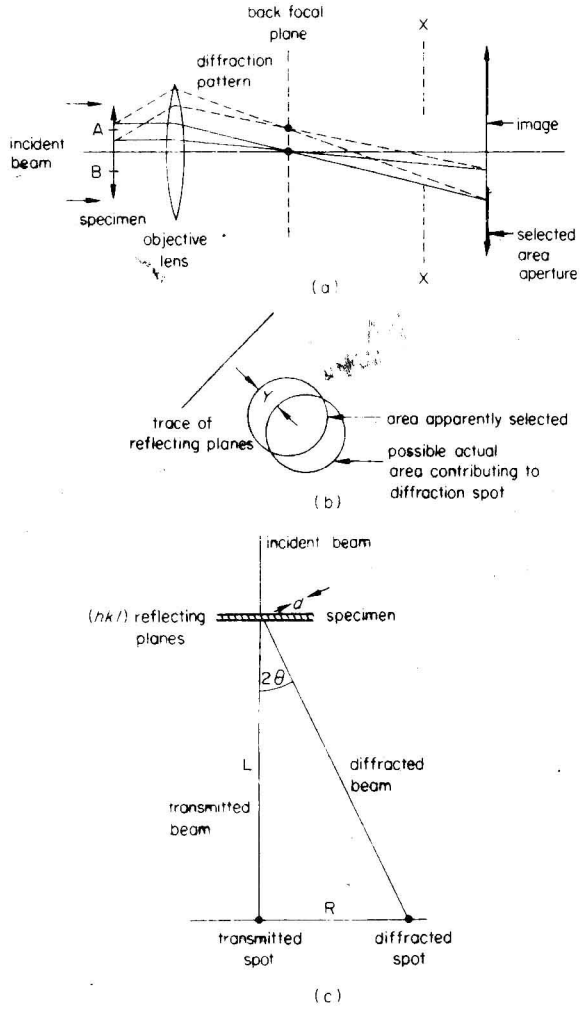

Figure 1.9 (a) Selected area diffraction using a selecting aperture in the plane of the image formed by the objective lens, (b) the influence of errors in microscope operation on the accuracy of area selection, (c) the diffraction camera construction to simulate the magnification of the diffraction pattern by the microscope lenses

Because both a diffraction pattern and an image of the specimen are always produced by the objective lens, a magnified image of either may be produced on the viewing screen by focussing the next lens in the magnification system on one or the other. The details of image and diffraction pattern formation are described below.

1.5.1 *Selected Area Diffraction*

It is essential to be able to form a diffraction pattern from a specific region of the specimen. The principles of this process, which is known as selected area diffraction (SAD), can be understood with reference to figure 1.9(a). Here there is an incident beam covering the specimen, and all transmitted and diffracted rays contribute to the diffraction pattern formed in the back focal plane of the objective lens, as described above. However, if an aperture is inserted coplanar with the image, only the transmitted and diffracted rays that originate within the region AB of the specimen are allowed into the remaining magnification system. Those from outside are not. Consequently, although all electrons from the specimen contribute to the diffraction pattern formed in the back focal plane of the objective lens, only those from the region AB are allowed to contribute to the diffraction pattern formed on the viewing screen.

The procedure for performing this SAD has been described by Agar (1960) and Phillips (1960), being based on the approach of Le Poole (1947). First, the lens below the selector aperture is focussed on it to produce an in-focus aperture image on the viewing screen. In the EM300/301 the diffraction lens* is used for this purpose. This is easier with the objective aperture withdrawn. The objective lens is then used to focus the image of the specimen on the viewing screen. For easier focussing the objective aperture may be inserted to improve image contrast. Thus an image is formed at the selector aperture level by the objective lens because this aperture is already in focus on the final screen. The last step is simply to remove the objective aperture and to reduce the strength of the diffraction lens until a focussed (minimum spot size) diffraction pattern appears on the final screen, that is the diffraction lens is focussed on the back focal plane of the objective lens. The focus of the diffraction pattern is best judged using the viewing binocular and with condenser 2 overfocussed by 1–2 steps on the coarse control.

It is important to realise that there can be significant errors in the selection procedure. Thus, if the image and selector aperture are not coplanar, rays from outside the region selected will contribute to the diffraction pattern. Such a situation would occur if the selector aperture were in position XX, figure 1.9(a), relative to the image plane. Furthermore, spherical aberration produces a curved image because the focal length of the objective lens changes across its aperture. Thus the image and selector aperture cannot be coplanar. The influence of these two factors on the accuracy with which a specific area may be selected may be discussed in terms of the Bragg law (section 2.2.2.1) in which a diffracted spot arises by reflection from a set of crystal planes oriented at a specific Bragg angle θ relative to the incident beam. The area from which a specific diffracted beam originates is displaced by a distance Y, figure 1.9(b), perpendicular to the trace of the reflecting planes† and given by

$$Y = D(2\theta) + C_s(2\theta)^3 \qquad (1.10)$$

* In a microscope with a three-lens magnification system the intermediate lens is used.
† That is parallel to the $\mathbf{g}$ vector (the line joining the transmitted and diffracted spot, see section 2.2.3).

where D is the distance by which the objective lens is out of focus. Thus, as the Bragg angle increases so does the inaccuracy of area selection. Consider a (220) reflection in a **B** [111] diffraction pattern. The value for $2\theta = 0.0297$ rad, and for a typical microscope $C_s = 3.5$ mm while the minimum focus step on the objective lens fine focus is 124 Å. Then $Y = 3.7 + 917$ Å ≈ 921 Å. In reality, however, it is only usual to focus the image using the medium control of the objective lens, which implies a value of $D \approx 3$ μm and a value of $Y = 1808$ Å.

From the above discussion it is clear that a reduction in the size of the selector aperture below that which selects an area $\lesssim 4000$ Å in diameter is not particularly useful, because the error in area selection can easily be equal to its radius. Finally, for really accurate work* it is important to adjust the microscope accurately.

It is also very important to realise that the action of the objective lens rotates the image 180° relative to the diffraction pattern. It is pointed out in section 2.2.3 and figure 2.9 that a vector $\boldsymbol{g}$ may be defined that is normal to the reflecting planes in the crystal and points from the transmitted to the reflected beam. The directions of $\boldsymbol{g}$ in object, image and diffraction pattern are shown in figure 1.10(a). Clearly the objective lens rotates $\boldsymbol{g}$ by 180° in the image but not the diffraction pattern relative to the object. This is a basic property of the objective lens and leads to the requirement for a 180° rotation between recorded images and diffraction patterns in some instruments, see section 1.11.3.

In conventional SAD with a three-lens magnification system, the intermediate lens is focussed on the diffraction pattern in the back focal plane of the objective lens. Because this lens is also used to alter the magnification of the image, SAD must be performed at one specific image magnification which may be incompatible with the scale of the microstructure to be investigated. However, if the microscope has a four-lens magnification system, the diffraction lens may be used to focus on the back focal plane of the objective lens, while the intermediate lens is responsible for changes in image magnification. Then SAD may be performed over a wide range of image magnification.

In general for SAD the microscope is operated with standard lens settings, so that the magnification of the diffraction pattern on the final screen is constant, except for the small variations discussed in section 1.11.2. The magnification factor is usually discussed in terms of an equivalent camera length that would be necessary to produce the same magnification in a conventional diffraction camera, that is without the lenses. This approach is shown schematically in figure 1.9(c) using the concept of reflection from crystal planes at the Bragg angle θ to generate the diffracted beam as described in section 2.2.2.1. If the distance from the transmitted to the diffracted spot on the plate is R, and the camera length is L, then $2\theta = R/L \approx 2 \sin \theta$ for small values of θ. Substituting in the Bragg relation equation (2.3) we have

$$Rd = \lambda L \tag{1.11}$$

where λL is the camera constant which describes the magnification of the diffraction pattern, and may be calibrated as described in section 1.11.2.

For a three-lens magnification system, the magnification of the diffraction pattern may only be varied over a limited range by changing the projector lens excitation because the intermediate lens excitation is fixed by the need to focus on the back focal plane of the objective lens. However, in the four-lens magnification system, a wide range of camera lengths may be produced because only the excitation of the diffraction lens remains constant while the intermediate and projector lenses can be used to change the magnification of the diffraction pattern.

For most purposes electron microscopes are operated at fixed lens settings equivalent to a standard camera length, usually 50–70 cm at 100 kV. However, for some purposes it may be convenient to use a different camera length. A smaller camera length (10–30 cm) enables more of the diffraction pattern to be viewed on the screen. It is useful if small format film (for example 70 mm) is used: for producing a Kikuchi map as described in section 2.7.3.3 and appendix 5; to ascertain that stray high-order reflections are not present when tilting the specimen to produce exact (for example two-beam) diffracting conditions; to observe Laue zones (see section 2.7.2.2); or for weak beam images with high-order reflections (see section 3.17).

A larger camera length 1–5 metres is useful to investigate the fine structure of the diffraction pattern described in sections 2.16–2.19. As the magnification increases exact focussing becomes more difficult. Consequently, the camera length should only be increased to a value such that the required measurements can be made directly on the plate, or to render visible the details of the pattern on a photographic enlargement. At large camera lengths most diffracted beams will not fall on the viewing screen; consequently the centred dark field technique described in section 1.5.2 must be used to move the diffracted spot of

* Diffraction patterns from small areas down to ~ 50 Å in diameter may now be obtained using scanning attachments that enable the incident beam diameter to be reduced to this value, for example Thompson (1973)

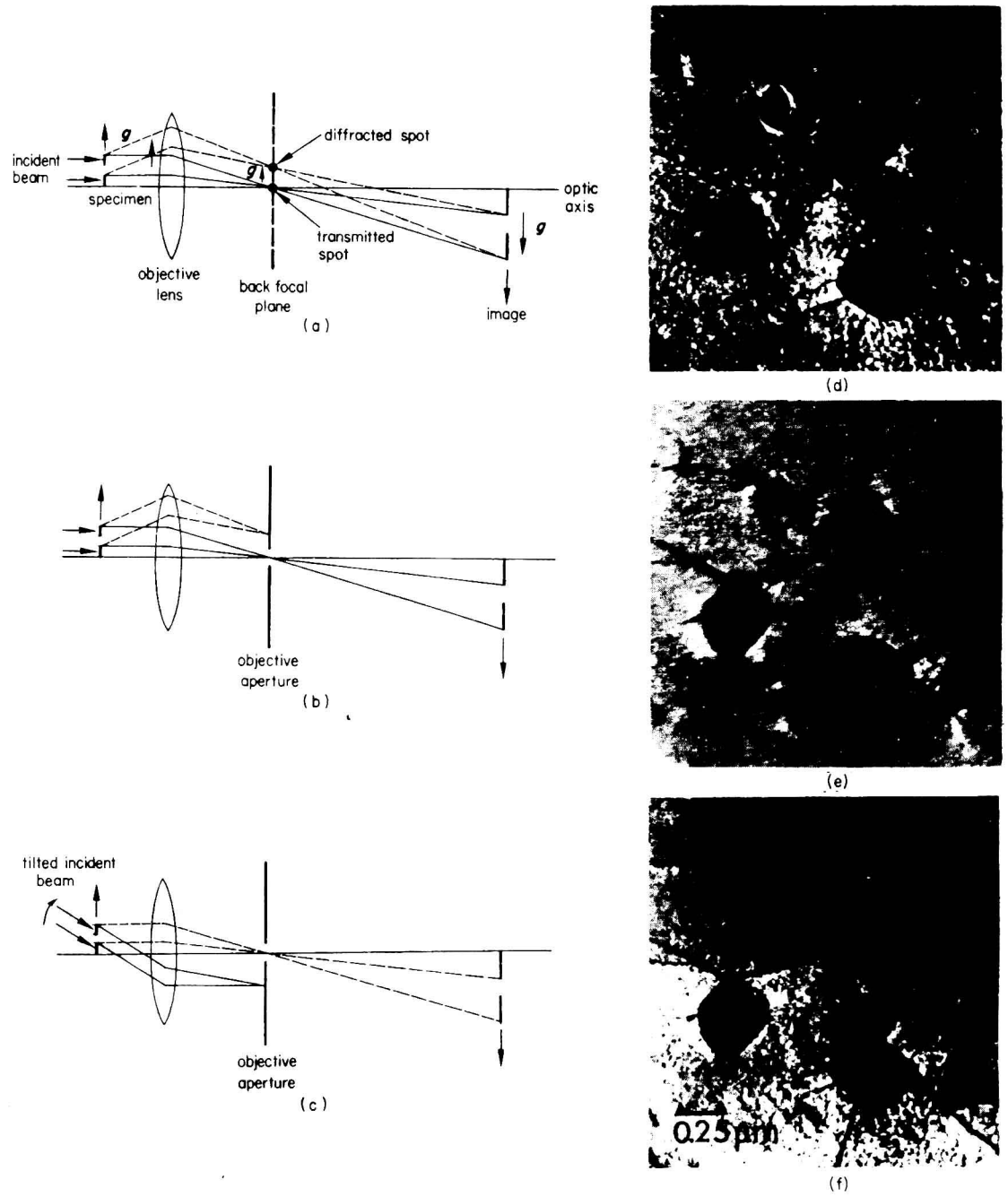

Figure 1.10 (a) The formation of a focussed diffraction pattern in the back focal plane of the objective lens, (b) the position of the objective aperture to form a bright field image, (c) tilted incident illumination to form a centred dark field image, (d) bright field, (e) displaced aperture dark field, (f) centred dark field of an aluminium grain in a Zn–40 wt% Al alloy. Dislocations and large zinc particles are visible [(d)–(f) Courtesy of A. Samuelsson]

interest to the optic axis. Under such circumstances the recommended procedure is to obtain centred dark field at the specific value of s* required using the spot of interest before increasing the camera length. The values of s required for different types of fine structure are described in sections 2.16–2.19. Finally, it is important to realise that detection of fine structure depends upon obtaining a fully focussed diffraction pattern correctly exposed, see section 2.17.1 for details. Two important points are relevant here. First, overexposure will prevent detection of fine structure. Second, details of the diffraction pattern that are invisible on the screen will be recorded on the plate. Consequently, a series of exposures will often be necessary to obtain the maximum amount of information from the pattern.

1.5.2 *Bright and Dark Field Images*

Bright field (BF) and centred dark field (CDF) are the most commonly used imaging modes for

* For definition see section 2.4, figure 2.16.

crystalline materials. Most of the analyses of crystal defects described in sections 3.4–3.9, 3.11–3.13, 3.22 involve comparison between, or detailed analysis of, BF and CDF images. Both types of image may be understood in terms of the image forming characteristics of the objective lens described above, figure 1.10(a).

A small aperture (5–70 μm diameter) may be inserted in the back focal plane of the objective lens to intercept the diffracted beam and only allow the transmitted beam to form an image. This situation is shown in figure 1.10(b) and is known as a BF image. Alternatively, the objective aperture could be displaced from the optic axis to intercept the transmitted beam and allow the diffracted beam to contribute to the image. This is known as a displaced aperture dark field, but a poor-quality image is produced because of the additional spherical aberration and astigmatism present when the electron path is not close to the optic axis. Compare figures 1.10(d), (e). In order to retain the resolution of the BF mode, the illumination incident on the specimen is tilted so that the diffracted electrons travel along the optic axis, see figure 1.10(c) and compare figures 1.10(e), (f). This technique is known as centred dark field (CDF) and is performed in older microscopes by mechanically tilting the electron gun, or in more modern microscopes by using an electromagnetic beam tilt device. CDF should always be used whenever it is necessary to observe the detail of a dark field image.

The procedure for forming a CDF image may be understood with reference to figure 1.11. Here the specimen has been tilted to produce two-beam conditions, that is the transmitted and only one diffracted beam. As shown in section 2.2.2.1 the diffraction process may be thought of as reflection by a set of crystal planes oriented at a specific Bragg angle θ relative to the incident beam. In figure 1.11(a) both the incident and transmitted beams lie on the optic axis but the diffracted beam does not and is intercepted by the objective

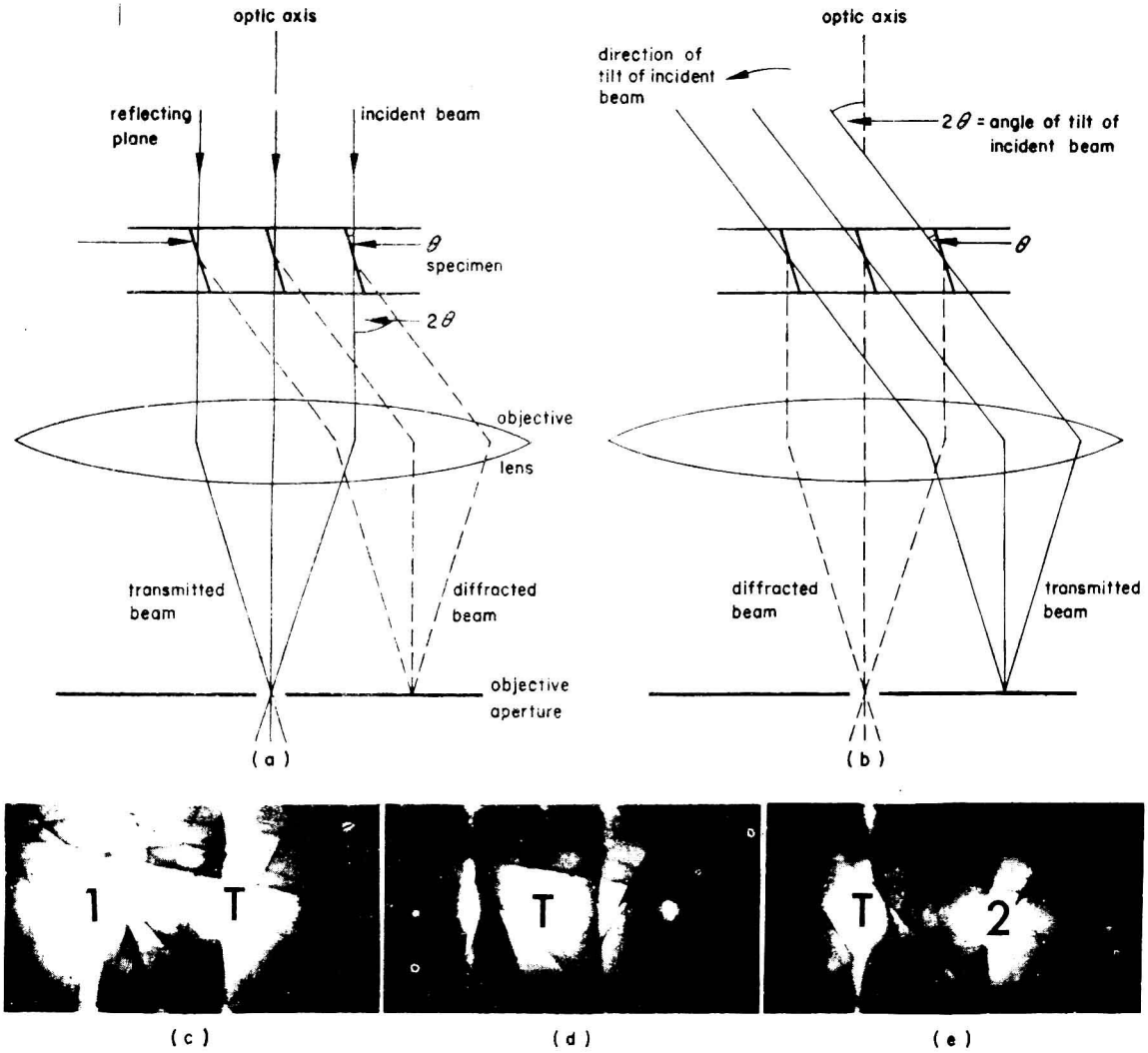

Figure 1.11 The relationship between the specimen reflecting planes and incident illumination for (a) BF and (b) CDF images, (c)–(e) the sequence of events occurring on the viewing screen during tilting of the incident illumination to form the CDF image in figure 1.10(f). The transmitted beam is labelled T and the diffracted beams 1 and 2 [(c)–(e) Courtesy of A. Samuelsson]

aperture (BF image). However, by tilting the beam through twice the Bragg angle (that is 2θ) reflection occurs from the other side of the same set of planes, figure 1.11(b). Thus the diffracted beam now lies on the optic axis while the transmitted beam follows the original path of the diffracted beam and is stopped by the objective aperture.

Remembering that the diffraction pattern on the viewing screen is simply a magnified image of that in the back focal plane of the objective lens, the sequence of events to perform CDF imaging is as follows.

(1) Produce a selected area diffraction pattern on the viewing screen, see section 1.5.1.

(2) Tilt the specimen until the spot of interest is bright (that is the Bragg law is satisfied), section 2.2.4.

(3) Operate the electromagnetic beam tilt controls (or the mechanical gun tilt if these are not available) to drive the transmitted spot into the position of the bright diffracted spot. This moves the weak diffracted spot opposite the original bright spot into the original position of the transmitted spot.* This point of coincidence may be judged by marking the original position of the transmitted beam using the beam stop.

(4) Refocus condenser 2 in the diffraction mode, centring the illumination where necessary, and return to the image mode.

(5) For maximum resolution the rotation centre of the objective lens may be adjusted in CDF image mode using the technique outlined previously in section 1.4.1 and the beam tilt controls employed to obtain CDF.

(6) If the microscope is provided with separate electromagnetic beam shift controls, for the beam tilt device, or, if the beam tilt controls can be independently aligned, it should be possible to switch directly from BF to CDF in the image mode and retain the images on the screen.

A typical sequence of events is shown in figure 1.11(c)–(e). Note that during beam tilting the original bright spot becomes steadily weaker while the opposite faint spot becomes brighter as the Bragg position is reached, see section 2.4. The BF and CDF images corresponding to figure 1.11(c) and (e) are shown in figures 3.2(d), (e). If the bright spot is moved to the centre it becomes progressively fainter because the Bragg angle is exceeded. Such a faint spot only produces a very faint image which will be almost invisible on the viewing screen. Thus it is necessary to tilt the specimen to make this spot bright again to produce a strong CDF image.

CDF imaging using specific diffraction spots is a very important and useful technique in analysing complicated diffraction patterns and in performing quantitative analysis of crystal defects. Each diffraction spot is produced by some diffraction process occurring at the specimen. Consequently the diffraction pattern contains all of the information concerning diffraction events from individual features of the specimen in the field of view. Therefore CDF imaging with each individual diffraction spot enables a direct correlation of the details of the image with those of the diffraction pattern.

Several examples of this approach are shown in sections 3.5.5, 3.6.2, 3.7.1, 3.8.1, 4.3.1, 4.9.2, 4.9.4, 4.11.1, 4.12.8, 4.13.2. The dark field analysis technique is also an important part of the techniques for quantitative analysis of crystal defects as discussed in sections 3.6, 3.8, 3.11–3.13.

1.5.3 *Weak Beam Images*

Weak beam (WB) images are formed in CDF using a faint diffraction spot, and have a higher resolution than conventional BF or CDF images. This technique has gained wide acceptance as a method of studying a variety of crystal defects, see section 3.17. It is essential to avoid any bright reflections in the diffraction pattern to simplify interpretation of the image. Under these circumstances resolution increases with increasing deviation from the Bragg reflecting position and it is known that high-resolution dislocation images require a value of $\dagger s \gtrsim 3 \times 10^{-2}$ Å^{-1}. The maximum usable specimen thickness is determined by the amount of inelastic scattering which destroys the contrast. Inelastic scattering depends on both material and the particular reflection. In copper with a {220} reflection the maximum useful thickness is ~800 Å for maximum resolution. However, thicker regions may be used in silicon for {111} reflections.

The simplest experimental method of obtaining a high-resolution WB image involves forming a CDF image with a first-order reflection while the bright Kikuchi line (section 2.6.3) lies well outside the third-order reflection. This may be achieved on any microscope but the procedure for one with electromagnetic beam tilt is shown below.

(1) Form a BF image of the region of interest and tilt the specimen to produce two beam reflecting conditions‡ with the reflection 1 of interest, see figure 1.12(a) in which the position of the optic axis is indicated by the dashed outline of the objective aperture.

(2) Check that the objective centre of rotation is

* In microscopes for which the beam tilt controls cannot be separately aligned, it may be necessary to defocus condenser 2.
† s is the parameter for describing the deviation from the Bragg reflection, see section 2.4.
‡ Only the diffracted spot of interest should be bright in the diffraction pattern.